

# A theoretical investigation for low-dimensional molecular-based magnetic materials

T Kaneyoshi and Y Nakamura

Department of Natural Science Informatics, School of Informatics and Sciences, Nagoya University, 464-01 Nagoya, Japan

Received 8 September 1997

**Abstract.** A two-dimensional ferromagnetic Ising system composed of ferrimagnetically ordered chains with alternating spin- $\frac{1}{2}$  and spin- $S$  ( $S > \frac{1}{2}$ ) atoms is investigated by the use of Ising spin identities and the differential operator technique, in order to clarify the magnetic properties of bimetallic molecular-based magnetic materials. The correlated effective-field approximation is used for the discussion. The numerical results of total magnetization  $M$  and inverse susceptibility  $\chi^{-1}$  are obtained and discussed for the two systems with  $S = 1$  and  $S = \frac{3}{2}$ . Some unexpected features are observed in the temperature dependences of  $\chi^{-1}$  when the crystal-field interaction constant  $d$  on a spin- $S$  atom becomes negative, such as the non-divergence of the  $\chi^{-1}$  in the systems with  $d = -1.0$ .

## 1. Introduction

A number of experimental works in the area of molecular-based magnetic materials has been stimulated in recent years and the magnetic properties, namely molecular magnetism, have become an important focus of scientific interest. Among them, bimetallic molecular-based magnetic materials in which two kinds of magnetic ion A and B regularly alternate have exhibited particularly interesting phenomena. These materials reveal the magnetic properties characteristic to the ferrimagnetic chains at high temperatures. At a transition temperature, some of them, such as  $\text{MnCu}(\text{pba-OH})(\text{H}_2\text{O})_3$ , show a three-dimensional ferromagnetic ordering of the ferrimagnetic chains and others, such as  $\text{MnCu}(\text{pba-OH})(\text{H}_2\text{O})_3 \cdot 2\text{H}_2\text{O}$ , exhibit a three-dimensional antiferromagnetic ordering of the ferrimagnetic chains. A perfect ferrimagnetic chain has also been synthesized in a bimetallic molecular-based material, such as  $\text{MnCu}(\text{opba})(\text{DMSO})_3$  [1].

On the other hand, several quantitative approaches to the magnetic properties of a ferrimagnetic chain have been discussed by the use of various theoretical methods (see [2]). Very recently, one of the present authors (TK) has discussed that the magnetic properties of a mixed spin Ising chain made up of two kinds of alternating magnetic atom, namely spin- $\frac{1}{2}$  A and spin- $S$  ( $S > \frac{1}{2}$ ) B atoms, can be obtained exactly by the use of the Ising spin identities and the differential operator technique [3]. The exact initial longitudinal and transverse susceptibilities of the system have been obtained in [4] and [5]. The thermodynamic properties (internal energy, spin correlation functions and specific heat) of the system have been solved exactly in [6]. In particular, when the crystal-field constant  $D$  on a spin- $S$  B atom is negative, the initial longitudinal susceptibility has shown a lot of new phenomena,

depending on whether the value of  $S$  is an integer or a half-integer. The specific heat has exhibited some characteristic (non-Schottky-type) features in the thermal variation, when the value of  $D$  takes a large negative value. As far as we know, however, the magnetic properties of the two-dimensional system composed of these Ising chains have not been discussed.

The aim of this work is to study the magnetic properties of a two-dimensional ferromagnetic system composed of mixed spin ferrimagnetic Ising chains within the framework of the correlated effective-field approximation (CEFA) [7], since the CEFA has reproduced the exact expressions of magnetic properties in a spin- $\frac{1}{2}$  Ising chain when the two-dimensional spin- $\frac{1}{2}$  Ising system with two anisotropic exchange interactions is decomposed into chains by cutting one of them [8]. In fact, the exact expressions of magnetic properties in the mixed spin Ising chain [4] can be also derived from this approach when the exchange interaction between nearest-neighbour chains is cut. The exact formulation of the system is given in section 2. In section 3, the expressions of the magnetic properties are discussed on the basis of the CEFA. The numerical results for the phase diagram and the temperature dependences of total magnetization and initial susceptibility are obtained and discussed in section 4.

## 2. General formulation

We consider a two-dimensional ferromagnetic Ising system composed of ferrimagnetically ordered chains with alternating spin- $\frac{1}{2}$  and spin- $S$  ( $S > \frac{1}{2}$ ) atoms described by the Hamiltonian

$$\mathcal{H} = J \sum_{(ij)} \mu_{i,j}^z S_{i+1/2,j}^z - J_1 \sum_{(ij)} \mu_{i,j}^z \mu_{i+1,j}^z - J_2 \sum_{(ij)} \mu_{i,j}^z \mu_{i,j+1}^z - D \sum_{(ij)} (S_{i+1/2,j}^z)^2 - H \sum_{(ij)} (\mu_{i,j}^z + S_{i+1/2,j}^z) \quad (1)$$

where the sites  $(i, j)$  and  $(i + \frac{1}{2}, j)$  represent the lattice points occupied by spin- $\frac{1}{2}$  and spin- $S$  atoms respectively in the  $j$ th chain,  $\mu_{i,j}^z$  takes the values of  $\pm \frac{1}{2}$  and the spin operator  $S_{i+1/2,j}^z$  can take the  $(2S + 1)$  values allowed for a spin  $S$  ( $S > \frac{1}{2}$ ). The first terms sum over only the nearest-neighbour pairs in the same chain.  $J$  ( $>0$ ) and  $J_1$  ( $>0$ ) are the intrachain exchange interactions.  $J_2$  ( $>0$ ) is the interchain exchange interaction.  $D$  is the crystal-field interaction constant.  $H$  is an applied magnetic field. The schematic representation of the system is described in figure 1. The total magnetization  $M_H$  of the system in an applied field  $H$  is given by

$$\frac{M_H}{N} = \sigma_H + m_H \quad (2)$$

with

$$\sigma_H = \langle \mu_{i,j}^z \rangle_H \quad m_H = \langle S_{i+1/2,j}^z \rangle_H \quad (3)$$

where  $N$  is the total number of spin- $\frac{1}{2}$  atoms in the chains and  $\langle \dots \rangle_H$  denotes the thermal average in the applied field. Note that in the following we write spin- $\frac{1}{2}$  and spin- $S$  atoms as  $\mu_i^z$  and  $S_j^z$  when it is not necessary to specify the chain in which those atoms are involved.

As discussed in [4] and [6], the magnetization  $m_H$  in a chain can be obtained exactly in a simple fashion by the use of Ising spin identifies and the differential operator technique:

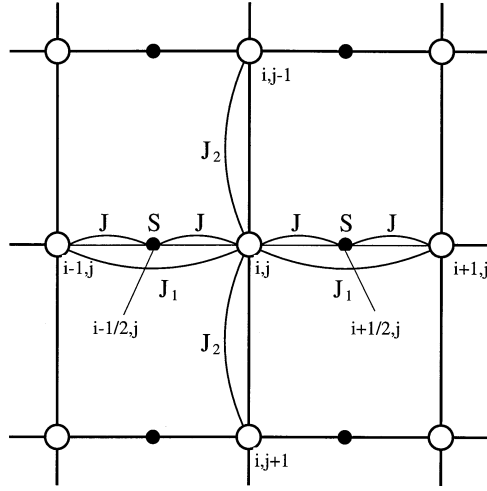


**Figure 1.** The spatial configuration of a two-dimensional ferromagnetic Ising system made up of two kinds of alternating magnetic atom. The white circles denote A atoms with  $S_A = \frac{1}{2}$  and the black circles represent B atoms with  $S_B = S$  ( $S > \frac{1}{2}$ ).  $J$ ,  $J_1$  and  $J_2$  are the exchange interactions.

$$m_H = \langle S_j^z \rangle_H = \cosh^2 \left( \frac{a}{2} \right) F_S(x+H)|_{x=0} - 2 \langle \mu_i^z + \mu_{i+1}^z \rangle_H \cosh \left( \frac{a}{2} \right) \\ \times \sinh \left( \frac{a}{2} \right) F_S(x+H)|_{x=0} + 4 \langle \mu_i^z \mu_{i+1}^z \rangle_H \sinh^2 \left( \frac{a}{2} \right) F_S(x+H)|_{x=0} \quad (4)$$

where  $a = J\nabla$  and  $\nabla = \partial/\partial x$  is the differential operator. The function  $F_S(x)$  depends on the value of  $S$ . The explicit expressions of  $F_S(x)$  are given in the appendix. In particular, when  $H = 0$ ,  $m_H$  reduces to

$$m = -2\sigma F_S(J) \quad (5)$$

with

$$m = \langle S_j^z \rangle_0 \quad \text{and} \quad \sigma = \langle \mu_i^z \rangle_0 \quad (6)$$

where  $\langle \cdot \cdot \rangle_0$  represents the thermal average in zero field. For the transformation from (4) to (5), it has been used that the function  $F_S(x)$  is an odd function of  $x$  and also the mathematical relation  $\exp(\alpha\nabla)\phi(x) = \phi(x+\alpha)$  has been applied. Thus, the total magnetization  $M$  in zero field is exactly given by

$$\frac{M}{N} = \sigma[1 - 2F_S(J)]. \quad (7)$$

Now, the initial susceptibility  $\chi$  of the present system is defined by

$$\chi = \left[ \frac{\partial}{\partial H} \left( \frac{M_H}{N} \right) \right]_{H=0} = \left( \frac{\partial \sigma_H}{\partial H} \right)_{H=0} + \left( \frac{\partial m_H}{\partial H} \right)_{H=0}. \quad (8)$$

Differentiating (4) with  $H$  and then taking  $H = 0$ , we obtain

$$\left( \frac{\partial m_H}{\partial H} \right)_{H=0} = \beta[\Delta_1 + 4 \langle \mu_i^z \mu_{i+1}^z \rangle_0 \Delta_2] - 2 \left( \frac{\partial \sigma_H}{\partial H} \right)_{H=0} F_S(J) \quad (9)$$

with

$$\Delta_1 = \frac{1}{2}[F_S^2(J) + F_S^1(0)] \quad \Delta_2 = \frac{1}{2}[F_S^2(J) - F_S^1(0)] \quad (10)$$

where the function  $F_S^1(x)$  is defined by

$$\left[ \frac{\partial}{\partial H} F_S(x+H) \right]_{H=0} = \beta F_S^1(x). \quad (11)$$

Substituting (9) into (8), the initial susceptibility  $\chi$  is exactly given by

$$\chi = \left( \frac{\partial \sigma_H}{\partial H} \right)_{H=0} [1 - 2F_S(J)] + \beta[\Delta_1 + 4\langle \mu_i^z \mu_{i+1}^z \rangle_0 \Delta_2]. \quad (12)$$

As is understood from (7) and (12), it is necessary to calculate  $\sigma$ ,  $(\partial \sigma_H / \partial H)_{H=0}$  and spin correlation functions (such as  $\langle \mu_i^z \mu_{i+1}^z \rangle_0$ ) in zero field, in order to discuss the  $M$  and  $\chi$  of the present system. In particular, when  $J_2 = 0$ , the problem reduces to that of an isolated ferrimagnetic Ising chain and the magnetic properties have been obtained exactly in [4] and [6].

### 3. Formulation of magnetic properties

The magnetization  $\sigma_H$  is defined by

$$\sigma_H = \langle \mu_i^z \rangle_H = \frac{\text{Tr} \mu_i^z e^{-\beta \mathcal{H}}}{\text{Tr} e^{-\beta \mathcal{H}}}. \quad (13)$$

In order to calculate  $\sigma_H$ , let us introduce the effective interaction  $J_{eff}^S(H)$  and the effective field  $H_{eff}$  between a pair of spins in a chain defined by

$$\begin{aligned} \sum_{S_j^z} \exp[-\beta J(\mu_i^z + \mu_{i+1}^z)S_j^z + \beta D(S_j^z)^2 + \beta H S_j^z] \\ = A \exp[\beta J_{eff}^S(H) \mu_i^z \mu_{i+1}^z + \beta H_{eff}(\mu_i^z + \mu_{i+1}^z)] \end{aligned} \quad (14)$$

like [4, 6, 9, 10]. The expressions of  $H_{eff}^S$  and  $J_{eff}^S(H)$  can be easily derived and are given for  $S = 1$  and  $S = \frac{3}{2}$  in [4–6]. Using (14), the Hamiltonian  $\mathcal{H}$  in (13) can be replaced by the effective Hamiltonian  $\mathcal{H}_{eff}$  defined as

$$\mathcal{H}_{eff} = -J_R(H) \sum_{i,j} \sum_{\delta} \mu_{i,j}^z \mu_{i,j+\delta}^z - H_R \sum_{i,j} \mu_{i,j}^z - J_2 \sum_{(i,j)} \mu_{i,j}^z \mu_{i,j+1}^z \quad (15)$$

with

$$H_R = H + 2H_{eff}^S \quad J_R(H) = J_1 + J_{eff}^S(H). \quad (16)$$

Thus, the investigation of  $\sigma_H$  reduces to the problem of the two-dimensional spin- $\frac{1}{2}$  Ising ferromagnet with anisotropic exchange interactions, namely the intrachain interaction  $J_R(H)$  and the interchain interaction  $J_2$ .

According to the Ising spin identifies and the differential operator technique, the magnetization  $\sigma_H$  can be written exactly in the form

$$\begin{aligned} \sigma_H = \langle \mu_i^z \rangle_H = \left\langle \prod_{\delta} \left[ \cosh \left( \frac{b}{2} \right) + 2\mu_{i+\delta}^z \sinh \left( \frac{b}{2} \right) \right] \right. \\ \left. \times \prod_{\delta'} \left[ \cosh \left( \frac{c}{2} \right) + 2\mu_{i+\delta'}^z \sinh \left( \frac{c}{2} \right) \right] \right\rangle_H f(x+H_R)|_{x=0} \end{aligned} \quad (17)$$

when  $b = J_R(H)\nabla$ ,  $c = J_2\nabla$  and the function  $f(x)$  is defined by

$$f(x) = \frac{1}{2} \tanh \left( \frac{\beta}{2} x \right). \quad (18)$$

$\delta$  and  $\delta'$  express respectively taking the nearest-neighbour sites in a chain and the sites in different nearest-neighbour chains. Furthermore, the identity (17) is generalized to

$$\begin{aligned} \langle g_i \mu_i^z \rangle_H &= \left\langle g_i \prod_{\delta} \left[ \cosh\left(\frac{b}{2}\right) + 2\mu_{i+\delta}^z \sinh\left(\frac{b}{2}\right) \right] \right. \\ &\quad \left. \times \prod_{\delta'} \left[ \cosh\left(\frac{c}{2}\right) + 2\mu_{i+\delta'}^z \sinh\left(\frac{c}{2}\right) \right] \right\rangle_H f(x + H_R)|_{x=0} \end{aligned} \quad (19)$$

where  $g_i$  can take any function of the Ising variables as long as it is not a function of the site  $i$ .

At this point, let us introduce the decoupling approximation and the correlated effective-field treatment for intrachain spin correlations, in order to calculate (17) and (19) approximately. The reason is based on the following facts. Firstly, in order to derive the exact expressions for magnetic properties in the ferrimagnetic Ising chain, the decoupling approximation is introduced for the interchain spin correlations:

$$\begin{aligned} \sigma_H &= \left\langle \prod_{\delta} \left[ \cosh\left(\frac{b}{2}\right) + 2\mu_{i+\delta}^z \sinh\left(\frac{b}{2}\right) \right] \right\rangle_H \\ &\quad \times \prod_{\delta'} \left[ \cosh\left(\frac{c}{2}\right) + 2\sigma_H \sinh\left(\frac{c}{2}\right) \right] f(x + H_R)|_{x=0} \end{aligned} \quad (20)$$

and

$$\begin{aligned} \langle g_i \mu_i^z \rangle_H &= \left\langle g_i \prod_{\delta} \left[ \cosh\left(\frac{b}{2}\right) + 2\mu_{i+\delta}^z \sinh\left(\frac{b}{2}\right) \right] \right\rangle_H \\ &\quad \times \prod_{\delta'} \left[ \cosh\left(\frac{c}{2}\right) + 2\sigma_H \sinh\left(\frac{c}{2}\right) \right] f(x + H_R)|_{x=0} \end{aligned} \quad (21)$$

where  $g_i$  is a function of spin- $\frac{1}{2}$  operators in the chains, such as  $g_i = \mu_{i+\delta}^z$ . Next, in order to treat the intrachain spin correlations of (20) and (21), let us introduce the correlated effective-field treatment

$$\mu_{i+\delta}^z = \sigma_H + \lambda(H)(\mu_i^z - \sigma_H) \quad (22)$$

since it has been proved that the exact expressions of magnetic properties in a spin- $\frac{1}{2}$  Ising chain can be derived from the approach [8]. In fact, we can obtain

$$\langle \mu_{i-1}^z \mu_{i+1}^z \rangle_H = \sigma_H^2 + \lambda_H^2 \left(\frac{1}{4} - \sigma_H^2\right) \quad (23a)$$

$$\langle \mu_i^z \mu_{i+1}^z \rangle_H = \sigma_H^2 + \lambda_H \left(\frac{1}{4} - \sigma_H^2\right) \quad (23b)$$

for the spin correlations in a chain, when (22) is applied. Here, the correlated effective-field parameter  $\lambda_H$  can be determined by substituting  $g_i = \mu_{i+\delta}^z$  into (21) and using the relation (23b), as discussed in [7].

Using (20) and (23a), the magnetization  $\sigma$  at  $H = 0.0$  is given by

$$\sigma = 4\sigma(K_1 + K_2) + 16\sigma^3(K_3 + K_4) + 16\sigma\lambda^2\left(\frac{1}{4} - \sigma^2\right)K_3 \quad (24)$$

with

$$\begin{aligned} K_1 &= \cosh^2(c/2) \sinh(b_0/2) \cosh(b_0/2) f(x)|_{x=0} \\ K_2 &= \cosh^2(b_0/2) \sinh(c/2) \cosh(c/2) f(x)|_{x=0} \\ K_3 &= \sinh^2(b_0/2) \sinh(c/2) \cosh(c/2) f(x)|_{x=0} \\ K_4 &= \sinh^2(c/2) \sinh(b_0/2) \cosh(b_0/2) f(x)|_{x=0} \end{aligned} \quad (25)$$

where  $b_0 = J_R \nabla$  with

$$J_R = J_1 + J_{eff}^S(H=0). \quad (26)$$

The correlated effective-field parameter  $\lambda$  ( $=\lambda_{H=0}$ ) at  $H = 0.0$  can be determined from (21) and (23b) as follows.

$$\begin{aligned} \sigma^2 + \lambda\left(\frac{1}{4} - \sigma^2\right) &= \frac{1}{2}K_1 + 2[\sigma^2 + \lambda^2\left(\frac{1}{4} - \sigma^2\right)]K_1 + 4\sigma^2(K_2 + K_3) + 2\sigma^2K_4 \\ &+ 8\sigma^2[\sigma^2\lambda^2\left(\frac{1}{4} - \sigma^2\right)]K_4. \end{aligned} \quad (27)$$

Thus, the temperature dependences of  $\sigma$  and  $\lambda$  can be determined by solving the coupled equations (24) and (25) numerically.

The transition temperature  $T_c$  of the two-dimensional system with  $J_2 \neq 0$  can be obtained by taking only the linear terms of  $\sigma$  in (24):

$$1 = 4(K_1 + K_2) + 4\lambda_c^2 K_3. \quad (28)$$

Here, the correlated effective-field parameter  $\lambda_c$  at  $T = T_c$  is

$$\lambda_c = \tanh\left(\frac{\beta_c}{4} J_R\right) \quad (29)$$

with  $\beta = 1/k_B T_c$ , since (27) becomes the quadratic equation of  $\lambda$  when substituting  $\sigma = 0$  and the physical solution is given by (29).

Now, in order to obtain the initial susceptibility  $\chi$  of the present system, it is necessary to calculate  $(\partial\sigma_H/\partial H)_{H=0}$  in (12). By differentiating (20) with  $H$  and using the relation (23a), it is given by

$$\begin{aligned} \left(\frac{\partial\sigma_H}{\partial H}\right)_{H=0} &= \frac{\beta}{4} \left[ 1 + 2\left(\frac{\partial H_{eff}^S}{\partial H}\right)_{H=0} \right] [\Delta_3 + 4\sigma^2(\Delta_4 + \Delta_6) + 16\sigma^2(\Delta_5 + \sigma^2\Delta_7)] \\ &+ 4\lambda^2\left(\frac{1}{4} - \sigma^2\right)(\Delta_4 + 4\sigma^2\Delta_7) + 4\left(\frac{\partial\sigma_H}{\partial H}\right)_{H=0} [K_1 + K_2 + K_3\lambda^2 \\ &+ 12\sigma^2K_4 + 12\sigma^2(1 - \lambda^2)K_3] + 32\lambda\sigma K_3 \left(\frac{\partial\lambda_H}{\partial H}\right)_{H=0} \left(\frac{1}{4} - \sigma^2\right) \end{aligned} \quad (30)$$

with

$$\begin{aligned} \Delta_3 &= \cosh^2(b_0/2) \cosh^2(c/2) \operatorname{sech}^2((\beta/2)x)|_{x=0} \\ \Delta_4 &= \cosh^2(c/2) \sinh^2(b_0/2) \operatorname{sech}^2((\beta/2)x)|_{x=0} \\ \Delta_5 &= \cosh(c/2) \sinh(c/2) \cosh(b_0/2) \sinh(b_0/2) \operatorname{sech}^2((\beta/2)x)|_{x=0} \\ \Delta_6 &= \cosh^2(b_0/2) \sinh^2(c/2) \operatorname{sech}^2((\beta/2)x)|_{x=0} \\ \Delta_7 &= \sinh^2(b_0/2) \sinh^2(c/2) \operatorname{sech}^2((\beta/2)x)|_{x=0}. \end{aligned} \quad (31)$$

Furthermore, one should notice that from the expression of  $H_{eff}^S$  defined by (14) we can obtain

$$\left(\frac{\partial H_{eff}^S}{\partial H}\right)_{H=0} = -F_S(J). \quad (32)$$

Using (21) with  $g_i = \mu_{i+1}^z$  and (23b), the factor  $(\partial\lambda_H/\partial H)_{H=0}$  in (30) is also given by the following form

$$(1 - 4\sigma^2) \left(\frac{\partial\lambda_H}{\partial H}\right)_{H=0} = \beta[1 - 2F_S(J)]U_1 + 4\left(\frac{\partial\sigma_H}{\partial H}\right)_{H=0} U_2 \quad (33)$$

with

$$U_1 = \frac{Q_2}{Q_1} \quad \text{and} \quad U_2 = \frac{Q_3}{Q_1} \quad (34)$$

where the coefficients  $Q_i$  ( $i = 1, 2, 3$ ) are given by

$$\begin{aligned} Q_1 &= 1 - 4\lambda(K_1 + 4\sigma^2 K_4) \\ Q_2 &= \sigma[\Delta_3 \Delta_4 + 2\Delta_5\{1 + \lambda^2 + 4\sigma^2(1 - \lambda^2)\} + 4\sigma^2(\Delta_6 + \Delta_7)] \\ Q_3 &= 2\sigma[4(K_2 + K_3) + 2K_4(1 + \lambda^2) + 2K_1(1 - \lambda^2) + 16\sigma^2 K_4(1 - \lambda^2) - (1 - \lambda)]. \end{aligned} \quad (35)$$

From (33) and (30), we obtain

$$\left(\frac{\partial \sigma_H}{\partial H}\right)_{H=0} = \frac{\beta}{4}[1 - 2F_S(J)] \frac{V_2}{1 - 4V_1} \quad (36)$$

with

$$\begin{aligned} V_1 &= K_1 + K_2 + K_3 \lambda^2 + 12\sigma^2 K_4 + 12\sigma^2(1 - \lambda^2)K_3 + 8\lambda\sigma K_3 U_2 \\ V_2 &= \Delta_3 + 4\sigma^2(\Delta_4 + \Delta_6) + 16\sigma^2(\Delta_5 + \sigma^2 \Delta_7) \\ &\quad + \lambda^2(1 - 4\sigma^2)(\Delta_4 + 4\sigma^2 \Delta_7) + 32\lambda\sigma K_3 U_1. \end{aligned} \quad (37)$$

Thus, the initial susceptibility  $\chi$  of the present system is given, from (36), (12) and (23b), by

$$\chi = \frac{\beta}{4}[1 - 2F_S(J)]^2 \frac{V_2}{1 - 4V_1} + \beta[\Delta_1 + \Delta_2\{\lambda + 4\sigma^2(1 - \lambda)\}] \quad (38)$$

where the  $\sigma$  and  $\lambda$  in (38) are given by solving the coupled equations (24) and (27).

At this point, when the system is paramagnetic or  $\sigma = 0$  for  $T > T_c$ , the paramagnetic susceptibility  $\chi_{para}$  is given by

$$\chi_{para} = \frac{\beta}{4}[1 - 2F_S(J)]^2 \frac{\Delta_3 + \lambda^2 \Delta_4}{1 - 4(K_1 + K_2 + K_3 \lambda^2)} + \beta[\Delta_1 + \Delta_2 \lambda] \quad (39)$$

with

$$\lambda = \tanh\left(\frac{\beta}{4} J_R\right). \quad (40)$$

The  $\chi_{para}$  exhibits the divergence at  $T = T_c$  determined from (28). In particular, when  $J_2 = 0$ , we can easily prove that (39) reproduces the exact expression (or (12)) of the initial susceptibility in an isolated ferrimagnetic Ising chain. Thus, the decoupling approximation ((20) or (21)) and the correlated effective-field treatment (22) derive the reasonable results for the magnetic properties of the present system.

#### 4. Numerical results

In this section, let us examine the magnetic properties of the two-dimensional ferromagnetic Ising system composed of ferrimagnetically ordered chains by solving the relations given in the previous sections numerically. In order to study them, the two values of  $S$ , namely  $S = 1$  and  $S = \frac{3}{2}$ , are taken here and the following parameters

$$\alpha = \frac{J_1}{J} \quad \gamma = \frac{J_2}{J} \quad d = \frac{D}{J} \quad (41)$$

are used for the numerical analyses.

## 4.1. Phase diagrams

From (7), there may be a compensation temperature  $T_k$  at which the total magnetization  $M$  reduces to zero even  $\sigma \neq 0$ . The compensation point in the system is exactly given by

$$1 = 2F_S(J). \quad (42)$$

Let us first study the phase diagrams (the variations of the transition temperature  $T_c$  and the  $T_k$ ) by solving the relations (28) and (42) numerically.

Figure 2(A) and (B) shows the variations of  $T_c$  and  $T_k$  as a function of  $d$  for the two values of  $S$ , selecting the four typical sets of pair values  $(\alpha, \gamma)$ . The solid and dashed lines represent respectively the  $T_c$  and the  $T_k$ . Accordingly, in order that a compensation point may exist in the system with the fixed values of  $(\alpha, \gamma)$ , each solid curve must be higher than the dashed curve. A compensation point can be obtained in the system when the value of  $d$  is larger than  $d = -1.0$ . In particular, the relation (42) is equivalent to that in [10] for  $p = 0.5$  and the whole plots of (42) as a function of  $d$  are also given in figure 2 of [10] for the two values of  $S$ .

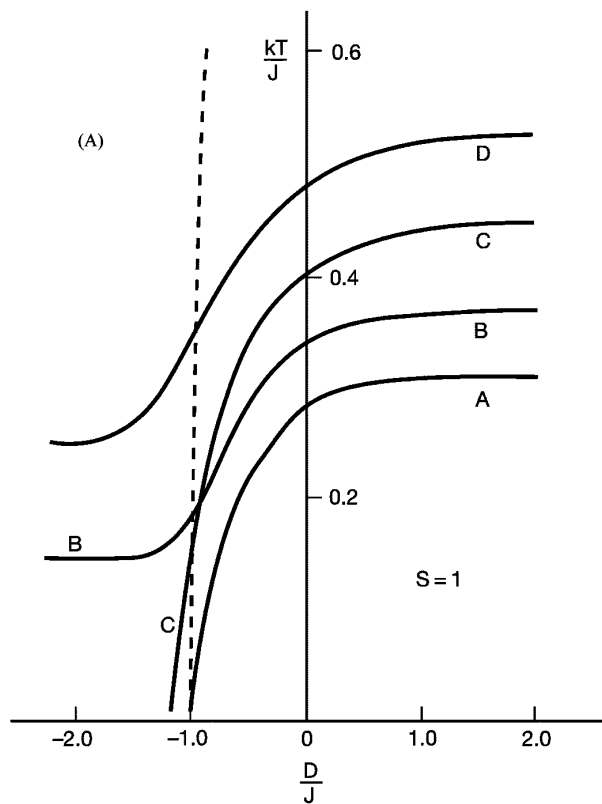


**Figure 2.** The phase diagram ( $T_c$  and  $T_k$ ) in the  $(T, D)$  space for the two-dimensional ferromagnetic Ising system composed of ferrimagnetically ordered chains, when the value of  $S$  is selected as  $S = 1$  in (A) or  $S = \frac{3}{2}$  in (B). The solid and dashed lines represent the  $T_c$  and the  $T_k$  (or the relation (42)), respectively. In each figure, the four sets of pair values  $(\alpha, \gamma)$  are selected for the numerical calculation:  $(\alpha, \gamma) = (0.0, 0.05)$  for the curve A,  $(0.5, 0.05)$  for the curve B,  $(0.0, 0.2)$  for the curve C and  $(0.5, 0.2)$  for the curve D.



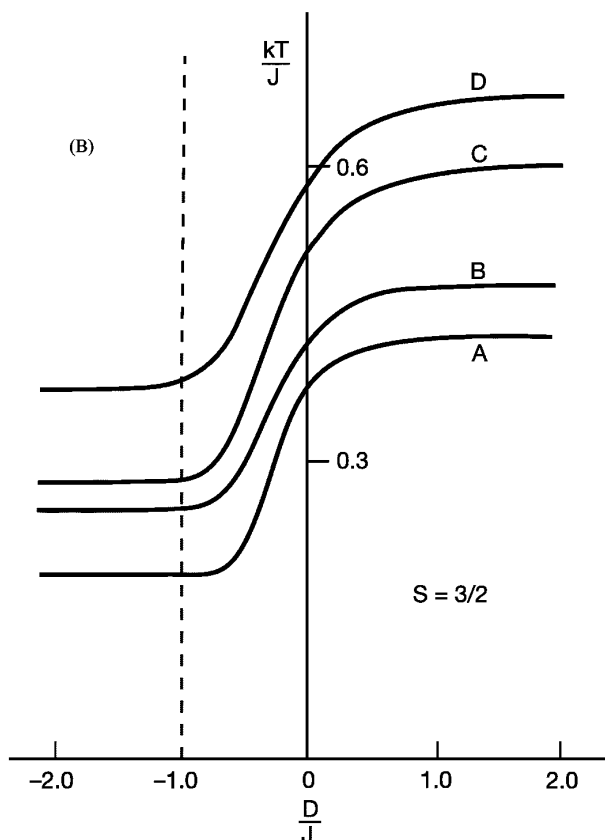
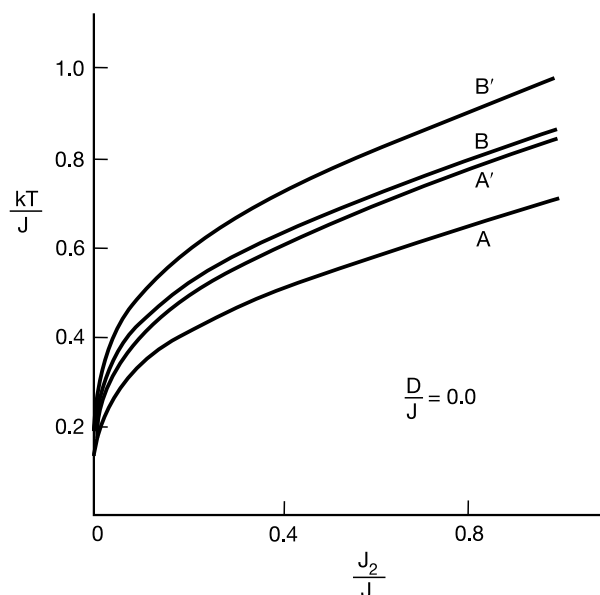


Figure 2. (Continued)

Comparing (A) and (B) of figure 2, a characteristic feature can be observed for the behaviour of the  $T_c$  in the system with  $\alpha = 0.0$ , depending on whether  $S$  is an integer ( $S = 1$ ) or a half-integer ( $S = \frac{3}{2}$ ). When  $S = 1$ , the  $T_c$  curves labelled A and C (or  $\alpha = 0.0$ ) seem to be going to zero in the vicinity of  $d = -1.0$ , although the values of  $T_c$  could not be determined accurately below  $k_B T/J < 0.01$  because of large numerical errors. When  $S = \frac{3}{2}$ , the  $T_c$  takes a finite constant value for  $d \ll -1.0$ . The difference comes from the following facts. When  $S = 1$  and  $d < -1.0$ , the spin of B atoms is in the  $S_j^z = 0$  state at  $T = 0$  K. On the other hand, when  $S = \frac{3}{2}$  and  $d < -0.5$ , the spin of B atoms is in the  $S_j^z = \pm \frac{1}{2}$  state at  $T = 0$  K. In other words, the magnetization of the system with  $S = 1$  and  $d < -1.0$  should be  $\sigma = m = 0.0$  at  $T = 0$  K, since B atoms in a chain behave like nonmagnetic atoms and no intrachain interaction connecting A atoms exists. When  $\alpha \neq 0.0$ , however, there exists a finite coupling  $J_1$  between a nearest-neighbour pair of A atoms even for  $d < -1.0$  and hence the behaviour of the  $T_c$  takes a form similar to that of  $S = \frac{3}{2}$ .

In figure 3, the  $T_c$  versus  $\gamma$  plots are given for the systems with  $S = 1$  and  $S = \frac{3}{2}$ , when the values of  $d$  is fixed at  $d = 0.0$  and the two values of  $\alpha$  are selected. In the region of  $\gamma < 0.1$ , the  $T_c$  reduces rapidly to zero with the decrease of  $\gamma$ . It is consistent with the prediction that the system with  $\gamma = 0.0$  is nothing but a collection of isolated Ising chains and the  $T_c$  must be zero.



**Figure 3.** The variation of  $T_c$  in the  $(T, J_2)$  space for the ferromagnetic system with  $D/J = 0.0$ , when the four sets of pair values  $(S, \alpha)$  are selected:  $(S, \alpha) = (1, 0.0)$  for the curve A,  $(1, 0.5)$  for the curve A',  $(\frac{3}{2}, 0.0)$  for the curve B and  $(\frac{3}{2}, 0.5)$  for the curve B'.

#### 4.2. Magnetization and initial susceptibility

Let us now examine the thermal variations of the total magnetization  $M$  and the initial susceptibility  $\chi$  in the two-dimensional ferromagnetic system composed of ferrimagnetically ordered Ising chains by solving the coupled equations (24) and (27) numerically. As is expected from the results of section 4.1, their temperature dependences will depend on whether the value of  $S$  is an integer ( $S = 1$ ) or a half-integer ( $S = \frac{3}{2}$ ) and may exhibit a lot of interesting features when the value of  $d$  becomes negative. Accordingly, some typical values of  $\alpha$ ,  $\gamma$  and  $d$  are taken from the phase diagrams in section 4.1.

Figure 4 shows the temperature dependences of  $|M|$  (or  $\sigma$ ) (solid line),  $k_B T \chi$  (dashed line) and  $\chi_{para}^{-1}$  (solid-dashed line) in the system with  $S = 1$ ,  $\alpha = 0.0$  and  $\gamma = 0.05$ , when the typical values of  $d$  are selected. In particular,  $k_B T \chi$  is plotted instead of  $\chi$ , since it is often used for the analyses of experimental data in molecular-based magnetic materials. In the figure, the  $|M|$  and the inverse paramagnetic susceptibility  $\chi_{para}^{-1}$  of the systems labelled A'', B'' and C'' ( $d = 1.0$ ,  $d = 0.0$  and  $d = -0.5$ ) exhibit the standard features in the thermal variations. The  $k_B T \chi$  for B' or C' ( $d = 0.0$  or  $d = -0.5$ ) shows a broad minimum in the temperature region of  $T > T_c$  observed for the bimetallic molecular-based magnetic materials [1, 2], exhibits divergence at  $T = T_c$  and decreases rapidly to a constant value at  $T = 0$  K. For the systems with  $d = -1.0$  (curve D or D') and  $d < -1.0$  (curve E'), on the other hand, some characteristic features can be observed in the magnetic properties.

When  $d < -1.0$ , the total magnetization  $|M|$  in the system with  $S = 1$  and  $\alpha = 0.0$  is given by  $|M| = 0.0$ , since the spin operator  $S_j^z$  of B atoms is firmly fixed at the  $S_j^z = 0$  state in the low-temperature region and hence  $\sigma = m = 0$  because  $J_1 = 0$ . Accordingly, the  $k_B T \chi$  in the system labelled E' ( $d = -2.0$ ) decreases monotonically from the high-temperature region, shows a broad minimum and then exhibits divergence in the vicinity of  $T = 0$  K. For the critical value of  $d = -1.0$  where the spin operator can change from the

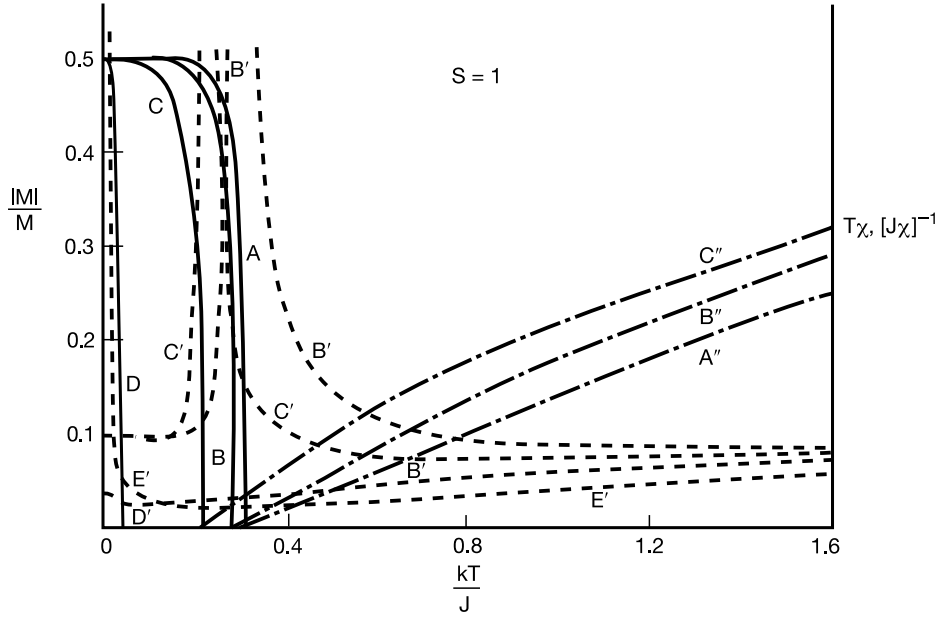


**Figure 4.** The thermal variations of the magnetic properties in the system with  $S = 1$ ,  $\alpha = 0.0$  and  $\gamma = 0.05$ , when the value of  $d$  is changed. The solid curves labelled A–C represent the temperature dependences of  $|M|$ , when  $d = 1.0$  (curve A),  $d = 0.0$  (curve B) and  $d = -0.5$  (curve C). But, solid curve D shows the temperature dependence of  $\sigma$  in the system with  $d = -1.0$  because  $|M| = 0$  for the whole temperature region. The solid-dashed curves A''–C'' denote the variation of inverse paramagnetic susceptibility in the system with  $d = 1.0$  (curve A''),  $d = 0.0$  (curve B'') and  $d = -0.5$  (curve C''). The dashed lines labelled B'–E' represent the temperature dependence of  $T\chi^{-1}$ , when the value of  $d$  is changed:  $d = 0.0$  for the curve B',  $d = -0.5$  for the curve C',  $d = -1.0$  for the curve D',  $d = -2.0$  for the curve E'.

$S_j^z = 0$  state to the  $S_j^z = \pm 1$  state at  $T = 0$  K, the magnetization  $m$  can take  $m = -1.0$  and  $m = 0.0$  with equal probability and it is given by the averaged value of  $m = -0.5$ . Owing to this fact, the total magnetization  $M$  is always given by  $m = 0.0$ , although the temperature dependence of  $\sigma$  exhibits the normal behaviour, as depicted in figure 4. Such a phenomenon is also expected from figure 2(A): when  $d = -1.0$ , the relation (42) is always satisfied and the compensation temperature  $T_c$  is given by  $T_c = 0$ . The  $k_B T\chi$  of the system labelled D' ( $d = -1.0$ ) shows behaviour similar to that of  $d = -2.0$  (curve E) in the high-temperature region. However, it does not exhibit the divergence in the vicinity of  $T = 0$  K but increases to a constant value at  $T = 0$  K. In particular, one should notice that the  $k_B T\chi$  in the system with  $d = -1.0$  does not exhibit the divergence at  $T = T_c$ , since the  $M$  is given by  $M = 0.0$ , being independent of  $T$  for  $T < T_c$  (or the relation (42) is satisfied in (39)).

In figure 4, the parameter  $\alpha$  (or the  $J_1$ ) was fixed at  $\alpha = 0.0$  and the temperature dependence of  $\chi$  in the system with  $S = 1$  and  $\gamma = 0.05$  did not express any unstable feature, even when  $d < -1.0$ . At this place, let us show one of the unexpected phenomena in the  $\chi$ - $T$  curve observed for the system with  $S = 1$ , when the value of  $\alpha$  is given by a finite value and the value of  $d$  becomes smaller than  $d = -1.0$ .

In order to compare with the results of figure 4, figure 5 shows the temperature dependences of  $|M|$  and the inverse susceptibility  $\chi^{-1}$  in the system with  $S = 1$ ,  $\alpha = 0.5$  and  $\gamma = 0.05$ , selecting three values of  $d$ , namely  $d = 0.0$ ,  $d = -1.0$  and  $d = -2.0$ . For

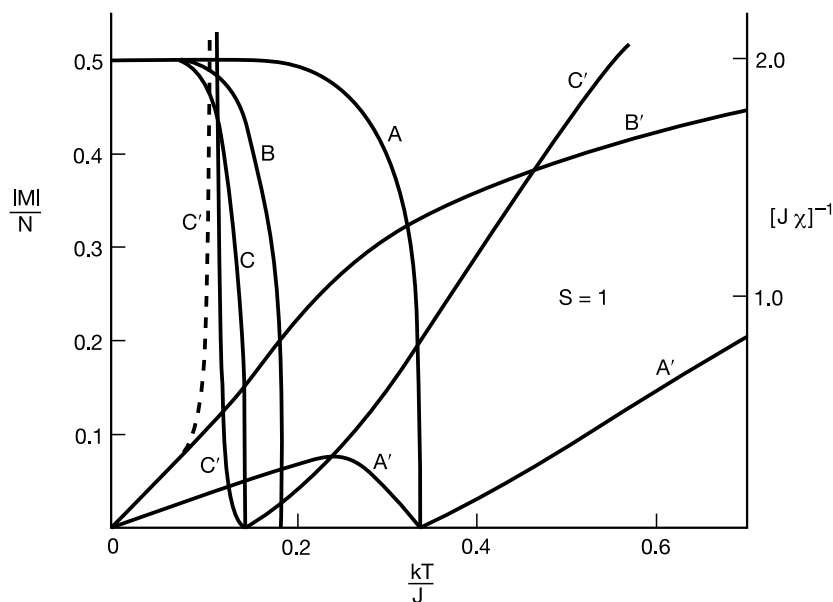


**Figure 5.** The temperature dependences of  $|M|$  (or  $\sigma$ ) and  $\chi^{-1}$  in the system with  $S = 1$ ,  $\alpha = 0.5$  and  $\gamma = 0.05$ , when the value of  $d$  is changed. The curves A and C represent the  $|M|$  for  $d = 0.0$  and  $d = -2.0$ , respectively. The curve B shows the temperature dependence of  $\sigma$  in the system with  $d = -1.0$  because  $|M| = 0$  in the whole temperature region. The curves A'–C' represent the temperature dependences of  $\chi^{-1}$  where  $d = 0.0$  (curve A'),  $d = -1.0$  (curve B') and  $d = -2.0$  (curve C'). Notice that the dashed line labelled C' represents the negative value of  $\chi^{-1}$  (or  $|\chi^{-1}|$ ) in the system with  $d = -2.0$  when  $T < T_c$ .

the system with  $d = -1.0$ , the temperature dependence of  $\sigma$  (curve B) is also plotted in the future, since the  $|M|$  is given by  $|M| = 0.0$ . The  $\chi^{-1}$  labelled B' ( $d = -1.0$ ) also does not exhibit the divergence at  $T = T_c$ , like the corresponding curve of  $k_B T \chi$  in figure 4. The temperature dependences of  $|M|$  and  $\chi^{-1}$  in the system with  $d = 0.0$  (curves A and A') express features similar to those of figure 4. For the system with  $d = -2.0$ , however, the temperature dependence of  $\chi^{-1}$  (curve C') exhibits an unexpected behaviour at a temperature below  $T_c$  (or the dashed line in the figure means that the  $\chi^{-1}$  becomes negative after showing the divergence), although the  $|M|$ – $T$  curve labelled C shows the normal behaviour because  $\alpha = 0.5$  and the  $\chi^{-1}$  takes the form expected for  $T > T_c$ . The reason is as follows. When  $d = -2.0$ , the spin operator of B atoms should be in the  $S_j^z = 0$  state at  $T = 0$  K. But, owing to  $J_1 \neq 0.0$ , the spin operator would like to be in the  $S_j^z = \pm 1$  state. Because of the competition, the  $\chi^{-1}$  may exhibit an unstable feature below  $T_c$ , but the  $|M|/N$  takes the value  $|M|/N = 0.5$  at  $T = 0$  K, even though the decoupling approximation introduced in (20) and (21) seems to be a good approximation for  $\gamma = 0.05$ .

The outstanding behaviour observed for the  $\chi^{-1}$ – $T$  curve labelled C' ( $d = -2.0$ ) in figure 5 is expected to be observed only for the system with an integer spin ( $S = 1$ ) because of the existence of the  $S_j^z = 0$  state. In fact, such a feature could not be found in the system with a half-integer spin ( $S = \frac{3}{2}$ ), as depicted in figure 6 where the  $\chi^{-1}$  versus  $T$  curves in the system with  $S = \frac{3}{2}$ ,  $\alpha = 0.5$  and  $\gamma = 0.05$  are plotted for five values of  $d$ .

In figure 6, the temperature dependences of  $|M|$  and  $\chi^{-1}$  in the system are plotted for three values of  $d$  ( $d = 0.0$ ,  $d = -0.5$  and  $d = -\frac{2}{3}$ ). When  $d > -0.5$ , the spin operator

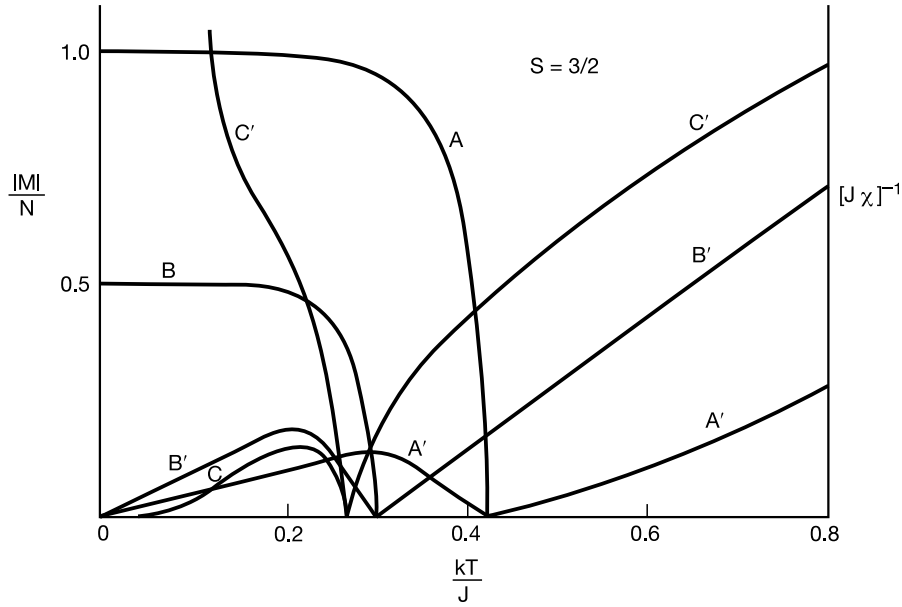


**Figure 6.** The temperature dependences of  $|M|$  and  $\chi^{-1}$  in the system with  $S = \frac{3}{2}$ ,  $\alpha = 0.5$  and  $\gamma = 0.05$ , when the value of  $d$  is changed. The curves A–C represent the  $|M|$ – $T$  curves for  $d = 0.0$  (curve A),  $d = -0.5$  (curve B) and  $d = -\frac{2}{3}$  (curve C). The curves A'–C' show the temperature dependences of  $\chi^{-1}$  in the system with  $d = 0.0$  (curve A'),  $d = -0.5$  (curve B') and  $d = -\frac{2}{3}$  (curve C').

of B atoms is in the  $S_j^z = \pm\frac{3}{2}$  state at  $T = 0$  K and hence the saturation magnetization of curve A is given by  $|M|/N = 1.0$ . At the critical value of  $d = -0.5$ , the spin operator takes the  $S_j^z = \pm\frac{3}{2}$  state and the  $S_j^z = \pm\frac{1}{2}$  state with equal probability and the saturation magnetization of curve B is given by  $|M|/N = 0.5$ , since  $\sigma = \frac{1}{2}$  and  $m = -1$  at  $T = 0$  K. When  $d < -0.5$ , the saturation magnetization of  $m$  is given by  $m = -0.5$ , so the total magnetization  $|M|$  of curve C starts to increase from zero at  $T = T_c$ , shows a broad maximum below  $T_c$  and reduces to zero at  $T = 0$  K. Because of this fact, the  $\chi^{-1}$  labelled C' ( $d = -\frac{2}{3}$ ) shows divergence when  $T$  goes to zero.

In figure 7, only the  $\chi^{-1}$ – $T$  curves are plotted for the systems with  $d = -1.0$  (curve A) and  $d = -2.0$  (curve B). They do not exhibit any unstable features in the thermal variation, in contrast to the  $\chi^{-1}$ – $T$  curve labelled C' ( $d = -2.0$ ) in figure 5, since the  $S_j^z = 0$  state is not allowed in the system with  $S = \frac{3}{2}$ . Finally, one should notice that the  $|M|$ – $T$  and  $\chi^{-1}$ – $T$  curves in the system with  $S = \frac{3}{2}$ ,  $\alpha = 0.0$  and  $\gamma = 0.05$  take forms similar to those of figure 6, although we will not show them.

## 5. Conclusions

In this work, we have investigated the magnetic properties of a two-dimensional ferromagnetic Ising system composed of ferrimagnetically ordered chains within the framework of the correlated effective-field approximation (CEFA) based on Ising spin identities and the differential operator technique. As discussed in section 3, the CEFA has derived the exact expressions of magnetization and initial susceptibility in [4] when the

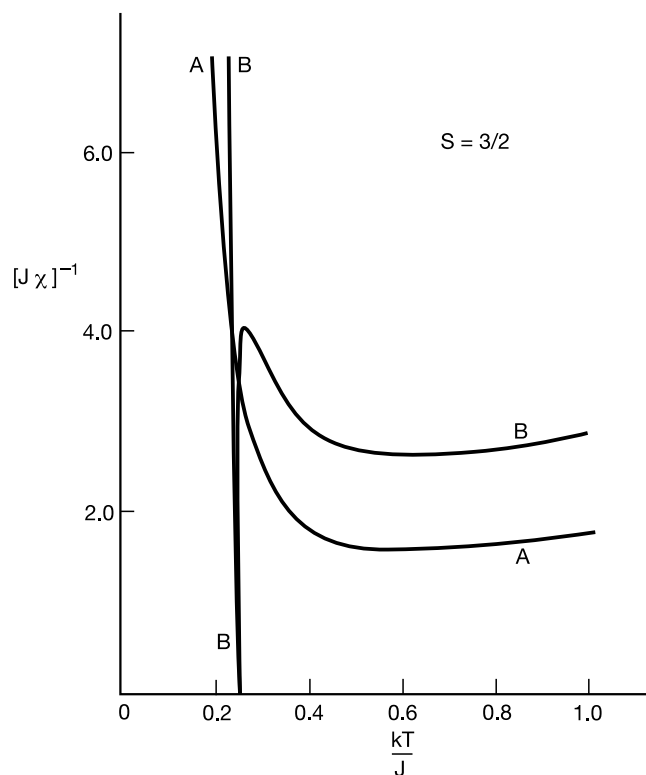


**Figure 7.** The temperature dependences of  $\chi^{-1}$  in the system with  $S = \frac{3}{2}$ ,  $\alpha = 0.5$  and  $\gamma = 0.05$ , when two negative values of  $d$  are selected:  $d = -1.0$  for the curve A and  $d = -2.0$  for the curve B.

interchain exchange interaction (or  $J_2$ ) is taken as  $J_2 = 0.0$  in the system. In section 4.1, the phase diagrams of the system have been examined numerically, selecting two values of  $S$  ( $S = 1$  and  $S = \frac{3}{2}$ ). When the intrachain exchange interaction  $J_1$  is taken as  $J_1 = 0.0$ , different features have been observed in figure 2 for the negative region of  $D$ , depending on whether the value of  $S$  is an integer ( $S = 1$ ) or a half-integer ( $S = \frac{3}{2}$ ), although the transition temperature of each system, as depicted in figure 3, reduces rapidly to zero with the decrease of  $J_2$ . In section 4.2, we have examined the temperature dependences of total magnetization  $M$  and initial susceptibility  $\chi$  in the system with  $S = 1$  or  $S = \frac{3}{2}$ , particularly selecting a weak interchain exchange interaction (or  $\gamma = 0.05$ ), in order to simulate the experimental data of bimetallic molecular-based magnetic materials [1]. In the process, two outstanding phenomena have been obtained in the  $\chi^{-1}$  versus  $T$  curves. (i) The  $\chi^{-1}$  of the system with  $d = -1.0$  does not exhibit divergence at  $T = T_c$ , which phenomenon is observed in both systems with  $S = 1$  and  $S = \frac{3}{2}$ . The reason comes from the fact that for the special value of  $d$  the relation (42) is always satisfied in (39). (ii) When  $\alpha \neq 0.0$ , the  $\chi^{-1}$  in the system with  $S = 1$  and  $d < -1.0$  becomes unstable (or negative) in the temperature region of  $T < T_c$ , although the  $|M|$ - $T$  curve shows the normal behaviour. Such a fact has been shown in figure 5 and discussed there. But, the phenomenon has not been observed in the  $\chi^{-1}$  of the system with  $S = \frac{2}{3}$ , as shown in figure 6. Thus, it may be interesting to study further whether the decoupling approximation introduced in (20) and

(21) is not appropriate for the system with  $S = 1$  and  $d < -1.0$ .

From the experimental point of view, the data of bimetallic molecular-based magnetic materials may be described by the Heisenberg model better than the present Ising model. Actually, Heisenberg models and Heisenberg Hamiltonians for such systems have in fact been studied in 1D using density matrix renormalization group (DMRG) [11, 12], quantum Monte Carlo and variational methods [13]. At the present stage, furthermore, it is not clear why type of interchain exchange interactions is mainly acting in the materials to show the three-dimensional ferromagnetic (or antiferromagnetic) ordering at a very low temperature. In this work, therefore, we have assumed that only the interchain exchange interaction  $J_2$  between nearest-neighbour A atoms is dominant for the ferromagnetic ordering. Even though some faults are included for the analyses of the experimental data, the results obtained in this work are extremely interesting. As shown in figure 4, the experimental data may be explained quantitatively from the present study.

Finally, we have here studied the two-dimensional ferromagnetic Ising system composed of ferrimagnetically ordered chains. The present formulation can be also extended to the case of the two-dimensional antiferromagnetic Ising system made up of ferrimagnetically ordered chains, although it is more complicated than the present one. The problem will be discussed in a separate work.

## Appendix

The function  $F_S(x)$  introduced in (4) is given by

$$F_S(x) = \frac{2 \sinh(\beta x)}{2 \cosh(\beta x) + \exp(-\beta D)} \quad (\text{A1})$$

for  $S = 1$ ,

$$F_S(x) = \frac{1}{2} \frac{3 \sinh(\frac{3}{2}\beta x) + \exp(-2\beta D) \sinh((\beta/2)x)}{\cosh(\frac{3}{2}\beta x) + \exp(-2\beta D) \cosh((\beta/2)x)} \quad (\text{A2})$$

for  $S = \frac{3}{2}$ , and so on.

## References

- [1] Kahn O 1996 *Molecular Magnetism: from Molecular Assemblies to the Devices* ed E Coronado *et al* (Dordrecht: Kluwer) p 243
- [2] Kahn O 1993 *Molecular Magnetism* (New York: VCH)
- [3] Kaneyoshi T 1993 *Acta Phys. Pol. A* **83** 703
- [4] Honmura R and Kaneyoshi T 1979 *J. Phys. C: Solid State Phys.* **12** 3979
- [5] Kaneyoshi T 1997 *Physica A* **237** 554
- [6] Kaneyoshi T 1997 *Prog. Theor. Phys.* **98** 57
- [7] Kaneyoshi T 1997 *Prog. Theor. Phys.* **97** 407
- [8] Kaneyoshi T, Filtipaldi I P, Honmura R and Manabe T 1981 *Phys. Rev. B* **24** 481
- [9] Kaneyoshi T and Tamura I 1982 *Phys. Rev. B* **25** 4679
- [10] Honmura R 1984 *Phys. Rev. B* **30** 348
- [11] Shoji I and Nakano H 1955 *Prog. Theor. Phys.* **13** 69
- [12] Shoji I 1972 *Phase Transitions and Critical Phenomena* vol 1, ed C Domb and M S Green (New York: Academic)
- [13] Kaneyoshi T 1996 *J. Phys.: Condens. Matter* **8** 4515
- [14] Pati S K, Ramasesha S and Sen D 1998 *Preprint cond-mat* 9704057
- [15] Pati S K, Ramasesha S and Sen D 1998 *Preprint cond-mat* 9610080
- [16] Miseska H J and Yamamoto S 1997 *Phys. Rev. B* **55** R3336